# Automatic Detection of Microvascular Obstruction in Patients with Myocardial Infarction

Trygve Eftestøl[1], Erlend Singsaas[2], Kjersti Engan[1], Leik Woie[2], Stein Ørn[2]

[1] Faculty of Science and Technology, University of Stavanger, Stavanger, Norway
[2] Department of Cardiology, Stavanger University Hospital, Stavanger, Norway

**Abstract**

*In this study we present a method for segmenting microvascular obstruction in patients with myocardial infarction. The presence of microvascular obstruction is an important prognostic indicator. In late enhanced cardiac magnetic resonance images scar will have very high signal intensity while areas of microvascular obstruction will appear with low signal intensity within the infarction.*

*The method was developed and tested on images from 22 patients. Candidate micriovascular regions within the scar were determined by using adaptive thresholding and training a classifier to distinguish true microvascular obstruction regions from false ones.*

*The best performing classifier (mean(std.dev.)) came out with true positive and negative rates of of 0.91(0.09), and 0.83(0.03) respectively.*

*The results of these preliminary experiments indicate that automatic detection of microvascular obstruction areas is feasible.*

## 1. Introduction

The presence and extent of microvascular obstruction (MO) in patients with acute myocardial infarction (MI) is an important prognostic indicator. In spite of successful opening of the large (epicardial) infarct related coronary artery, MO occurs in some patients due to damage and/or obstruction of the small blood vessels within the core of the MI. MO is most prominent in the early phase following MI. Following the healing of MI, microcirculation will gradually be restored in most patients[1].

In late Gadolinium (Gd) enhanced cardiac magnetic resonance images (LGE-CMRI), pixels within the MI will normally appear with very high signal intensity (SI) due to accumulation of Gd contrast agent within the infarcted myocardium. In contrast, SI is very low within regions of MO due to attenuation of Gd passage into this territory (figure 1).

In current image applications of LGE-CMRI where properties of the infarction are analysed, infarctions are defined as regions with pixels of high-SI. Since areas of MO have low SI, it is important to identify MO-regions if image analysis of LGE-CMRI is to be performed following acute MI[2]. Therefore we have designed an automatic method to detect MO-regions.

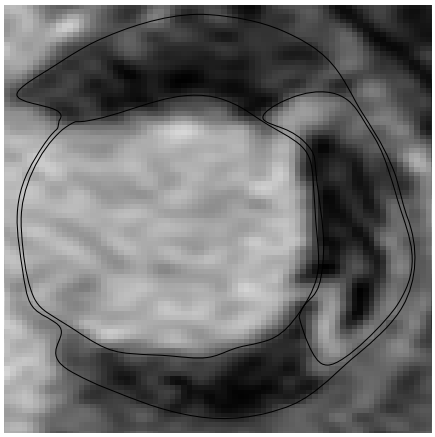

Figure 1. The figure shows a typical short axis of the left ventricle (LV). The inner- (IC) and outer contours (OC) of the myocardium and the myocardial infarction (MI) have been manually demarked. The areas of microvascular obstruction (MO) appears as areas of pixels with low signal intensity within the MI.

## 2. Material and methods

The scar and the inner- (IC) and the outer contours (OC) along the epicardial and endocardial boundaries in LGE-CMRI from 22 patients were manually traced. In short the mehod works as follows per 2D image slice: Candidate MO-regions within the scar were determined by areas

of pixels with SI values below a threshold adaptively determined from discriminative information in scar, normal appearing tissue and natural clusters within the scar. Each detected MO-region was then labelled by a cardiologist as a true (T) or false (F) MO as shown in figure 4 (where T/F corresponds to green/yellow numbering).

Each candidate MO region was characterised by features like area, centroid, orientation and some placement properties of the dilated area around the region. Different feature combinations were used to design a classifier for discriminating true from false MO-regions. In the classifier design both parametric and non-parametric classifiers were tested in a cross validation strategy.

## 2.1. Patients and images

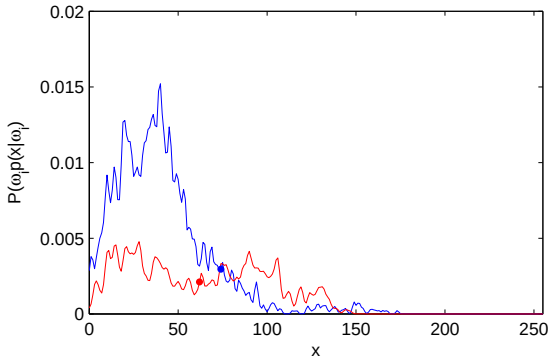


Figure 2. Estimated class specific probability density functions showing SI value distributions within scar (red) and in normal myocardium (blue). Thresholds $t_1$ and $t_2$ are shown in blue and red respectively.

The 22 patients included in this study were all admitted to hospital due to first-time acute ST-elevation myocardial infarction (STEMI). All patients were examined with coronary angiography during the acute phase, demonstrating single coronary artery disease, with a large coronary artery being occluded. All patients were subsequently successfully revascularized by primary percutaneous coronary intervention (PCI) without any residual stenosis. The patients underwent CMRI 2 days after PCI, using a 1.5 T Philips Intera R 8.3. A Gd based contrast agent, Omniscan, was administered intravenously at a dosage of 0.25 mmol/kg (at this dosage in order to reduce problems with early washout). LGE images were acquired 10-15 minutes later, using an inversion-recovery-prepared T1 weighted gradient-echo sequence with a typical pixel size of 0.82x0.82 mm2, covering the whole ventricle with short-axis slices of 10 mm thickness, without inter-slice gaps. Inversion recovery sequences were performed with individually adapted inversion times of 200 to 300 ms aiming to nullify normal myocardium. Subsequently, the CMRI-LGE images were processed in Matlab (MathWorks, Natick, Massachusetts, U.S.A.) with manually tracing of the epi- and endocardial boundaries of the left ventricle and delineation of the MI, performed by a cardiologist.

## 2.2. Determining SI value threshold

A combined approach was used to determine a threshold to discriminate MO pixels within the scar for a given patient. Let $x$ indicate the pixel position and $f(x)$ the SI value. First, a threshold, $t_1$ discriminating SI values in the myocardium outside the scar from those within the scar was determined by using a classification approach where the feature, $f(x)$, corresponds to the SI value. Each feature in the normal myocardium is assigned to class $\omega_1$ while those in the scar is assigned to $\omega_2$. The class specific density functions $\hat{p}(f(x)|\omega_i), i = 1, 2$ were estimated using the parzen window technnique with gaussian windows and window width $h_1 = 30$. The prior propbabilities where estimated as $\hat{P}(\omega_i) = n_i/(n_1 + n_2), i = 1, 2$ where $n_1$ and $n_2$ are the number of pixels in each of the two classes respectively. The threshold was defined as the lowest value $t_1$ of $f(x)$ for which

$$t_1 = \min_{f(x)} \left[ \hat{P}(\omega_2)\hat{p}(f(x)|\omega_2) > \hat{P}(\omega_1)\hat{p}(f(x)|\omega_1) \right]. \quad (1)$$

Second, the $k$-means clustering algorithm was used to distinguish between scar and MO tissue within the scar with $k = 2$, so that a pixel belongs to one of two clusters $C_i$, i=1,2. The threshold value $t_2$ was defines as

$$t_2 = \min_{f(x)} \left\{ \max[f(x)]_{f(x)\in C_1}, \max[f(x)]_{f(x)\in C_2} \right\}. \quad (2)$$

The combined threshold $t_t$ was determined in an ad hoc manner as

$$t_t = 0.5t_1 + 0.5t_2. \quad (3)$$

## 2.3. Characterising candidate MOs

Prior to the characterisation, some mask and morphological operations were performed to identify the candidate regions and to be able to determine vicinity to to the boundaries of the myocardium. The mask for the candidate MO was determined as the pixels within the scar region $MI$ satisfying

$$\text{MO}_{mask} = f(x) < t_t, x \in \text{MI}. \quad (4)$$

Furthermore $\text{MO}_{mask}$ is split into connected regions $\text{MO}_l$ so that

$$\text{MO}_{mask} = \cup_{l=1}^{L} \text{MO}_l, \quad (5)$$

where $L$ is the number of identified connected regions[3].

For each $\text{MO}_l$ a morphological dilation with a 2 pixel neighborhood diamond shaped structural element $D$ was performed so that

$$\text{MOD}_l = \text{MO}_l \oplus D \tag{6}$$

Furthermore, the belt around $\text{MO}_l$ is defined as

$$\text{B}_l = \text{MOD}_l - \text{MO}_l. \tag{7}$$

The part of the belt within the scar, within the myocardium and outside the myocardium is defined as $\text{B}_{ls} = \text{B}_l \cap MI$, $\text{B}_{lm} = \text{B}_l \cap MY$ and $\text{B}_{lo} = \text{B}_l \setminus MY$where MY is the myocardial region. Figure 3 shows three candidate MOs segmented within the scar where the pixels are shown in red. The pixels of the belt around each candidate MO are shown in green. Note how a bigger proportion of the belts of the smaller false MOs are positioned outside the scar.

To determine whether a region $\text{MO}_l$ is a true MO or not, it was characterised by calculating several features describing its shape, size and placement characteristics

$v_a$ : Number of pixels in $\text{MO}_l$ relative to the number of pixels in MI.

$v_c$ : The euclidean distance between the centroids of $\text{MO}_l$ and MI.

$v_o$ : The absolute value of the difference between the angle between the x-axis and the major axis of an ellipse fitted to the $\text{MO}_l$ region ($\angle MO_l$) and the corresponding angle of the MI region ($\angle MI$) so that $v_o = |\angle MO_l - \angle MI|$.

$N_b$ : Number of pixels in $\text{B}_l$.

$N_{bi}$ : Number of pixels in $\text{B}_{lm} \setminus \text{B}_{ls}$ (within nonscar region of myocardium).

$N_{bo}$ : Number of pixels in $\text{B}_{lo}$ (outside myocardium).

$v_{bi} = N_{bi}/N_b$ : Size of belt in nonscar region of myocardium relative to belt size.

$v_{bo} = N_{bo}/N_b$ : Size of belt outside myocardium relative to belt size.

## 2.4. Distinguishing between true and false MOs

A Bayes classifier was trained to classify a candidate MO as true ($\omega_T$) or false($\omega_F$). The feature vector $\mathbf{v}$ was constructed by combining a selection of $d$ features from the set

$$V = \{v_a, v_c, v_o, v_{bi}, v_{bo}\}, \tag{8}$$

$d$ being in the range 1 to 5. The class specific density functions $\hat{p}(\mathbf{v}|\omega_i), i = T, F$ were estimated using either maximum likelihood estimation, the parzen window technnique with gaussian windows with varying window widths or the $k_n$-nearest neighbor technique with varying $k_n$. The prior propbabilities where estimated as described in section 2.2. A candidate object was classified as MO if

$$\hat{P}(\omega_T)\hat{p}(\mathbf{v}|\omega_T) > \hat{P}(\omega_F)\hat{p}(\mathbf{v}|\omega_F). \tag{9}$$

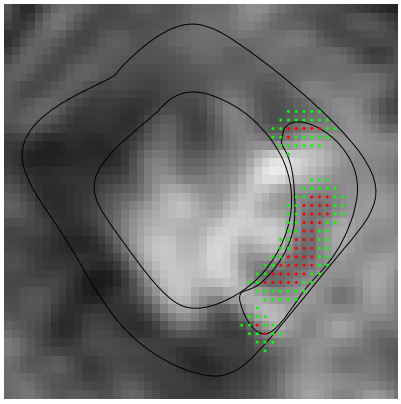

Figure 3. Original infarcted MRI with myocardium and scar manually delineated. Pixels in candidate MO-regions are shown in red while the added pixels resulting from dilation is shown in green.

## 3. Results

In 22 patients, 576 objects were manually labelled by consensus between an engineer and a cardiologist. In total 33 and 543 objects were labelled as true and false MOs respectively.

The classifier was trained by a bottom up approach choosing the best classifier with 1 feature, then finding the best 2D combination including this and thus increasing dimensionality. Cross validation with 3 folds were used.

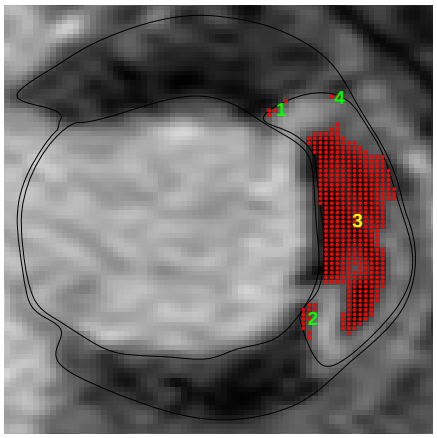


Figure 4. Original infarcted MRI with myocardium and scar manually delineated. Candidate MO-regions (red) detected as true (yellow numbers) or false (green numbers).

The best performance for each type of classifier is shown in Table 1. In the selection of features and training of the candidate classifiers, the Parzen classifier showed the best performance (mean(std.dev.)) with true positive and negative rates of 0.91(0.09), and 0.83(0.03) combining features 1,4, and 5. Combining all features worked best for ML and 1 and 5 for $k_n$ nearest neighbor.

Table 1. Best performing classifiers. Results are shown as mean(std.dev.) for true positive rate (TP) and true negative rate (TN).

| Classifier | TP | TN |
|---|---|---|
| Parzen, $h_n = 0.1$ | 0.91(0.09) | 0.83(0.03) |
| Maximum likelihood | 0.76(0.11) | 0.97(0.01) |
| Nearest neigh. $k_n = 1$ | 0.76(0.14) | 0.73(0.17) |

## 4. Discussion

This study demonstrates the feasability of segmenting areas of microvascular obstruction within the scarred area in LG enhanced cardiac MRI from patients with myocardial infarction.

The quantification of the size of MO has been identified as a significant marker for prognostification in patients with acute myocardial infarction[4, 5]. Size quantification of MO was not an objective of this study, but once the MO regions has been segmented, such quantification is straightforward, the number of pixels being the simplest such measure.

An important contribution by the current method is that it allows integration of MO territories into the assessment of infarcted myocardium in LGE-CMRI images. Previous methods for the assessment of myocardial scars cannot be applied to LGE-CMRI images acquired shortly following acute MI due to the high prevalence of MO during the first weeks following acute MI. The automatic identification of MO allows development of algorithms that permits interpretation of SI within the MO territory as well as the more peripheral areas of the infarcted myocardium.

In the current study, a limited dataset of only 22 patients were used for MO annotation. A future study should include more patients to make a larger dataset where a independent dataset should be kept isolated from the cross validation to yield a final performance score for the classifier.

The true negative rate of 0.83(0.03) indicates that a future study also should include more features to improve the accuracy further. Other types of classifiers might also be tried.

Another limitation of the current study is the fact that the scar was manually segmented by a cardiologist. An automatic method for scar segmentation would make the method less reliable of manual annotation work. Sevreal methods for scar segmentation might be relevant[6, 7]. Likewise, the endo- and epicardial boundaries were manually segmented, and fully automated methods might also be considered in future studies of automatic MO segmentation to be able to handle large data sets[8].

## 5. Conclusion

The results of these preliminary experiments indicate that automatic detection of MO areas is feasible. In future work, the method sshould be combined with automatic delineation of the scarred area, and the inner and outer boundaries of the myocardium.

## References


[1] Ørn S, Manhenke C, Greve OJ, et al. Microvascular obstruction is a major determinant of infarct healing and subsequent left ventricular remodelling following primary percutaneous coronary intervention. Eur Heart J 2009;30:1978–1985.

[2] Engan K, Eftestøl T, Ørn S, et al. Exploratory data analysis of image texture and statistical features on myocardium and infarction areas in cardiac magnetic resonance images. In Proc. EMBC. 2010; 5728 – 5731.

[3] Haralick RM, Shapiro LG. Computer and Robot Vision, volume 1. Reading, Massachusetts: Addison-Wesley, 1992.

[4] Wu KC, Zerhouni EA, Judd RM, Lugo-Olivieri CH, Barouch LA, Schulman SP, Blumenthal RS, Lima JA. Prognostic significance of microvascular obstruction by magnetic resonance imaging in patients with acute myocardial infarction. Circulation 1998;97(8):765–772.

[5] Rochitte CE, Lima JA, Bluemke DA, Reeder SB, McVeigh ER, Furuta T, Becker LC, Melin JA. Magnitude and time course of microvascular obstruction and tissue injury after acute myocardial infarction. Circulation 1998;98(10):1006–1014.

[6] Kotu LP, Engan K, Skretting K, Ørn S, Woie L, Eftestøl T. Segmentation of scarred myocardium in cardiac magnetic resonance images. ISRN Biomedical Imaging 2013;2013.

[7] Woie L, Måløy F, Eftestøl T, Engan K, Edvardsen T, Kvaløy JT, Ørn S. Comparing a novel automatic 3d method for lge-cmr quantification of scar size with established methods. The international journal of cardiovascular imaging 2014; 30(2):339–347.

[8] Engan K, Naranjo V, Eftesol T, Orn S, Woie L. Automatic segmentation of the epicardium in late gadolinium enhanced cardiac mr images. In Computing in Cardiology Conference (CinC), 2013. IEEE, 2013; 631–634.



Address for correspondence:

Trygve Eftestøl
University of Stavanger, N-4036 Stavanger, Norway
tel./fax: ++47-5183-2035/1750
trygve.eftestol@uis.no